Noise in digital and digital-analog quantum computation

Paula García-Molina, 1, 2, * Ana Martin, 1, 3 Mikel Garcia de Andoin, 1, 3, 4 and Mikel Sanz 1, 3, 5, †

¹Department of Physical Chemistry, University of the Basque Country UPV/EHU, Apartado 644, 48080 Bilbao, Spain

²Institute of Fundamental Physics, IFF-CSIC, Calle Serrano 113b, 28006 Madrid, Spain

³EHU Quantum Center, University of the Basque Country UPV/EHU, 48940 Leioa, Spain

⁴TECNALIA, Basque Research and Technology Alliance (BRTA), 48160 Derio, Spain

⁵IKERBASQUE, Basque Foundation for Science, Plaza Euskadi 5, 48009 Bilbao, Spain

Quantum computing uses quantum resources provided by the underlying quantum nature of matter to enhance classical computation. However, the current Noisy Intermediate-Scale Quantum (NISQ) era in quantum computing is characterized by the use of quantum processors comprising from a few tens to, at most, a few hundreds of physical qubits without implementing quantum error correction techniques. This limits the scalability in the implementation of quantum algorithms. Digital-analog quantum computing (DAQC) has been proposed as a more resilient alternative quantum computing paradigm to outperform digital quantum computation within the NISQ era framework. It arises from adding the flexibility provided by fast single-qubit gates to the robustness of analog quantum simulations. Here, we perform a careful comparison between the digital and digital-analog paradigms under the presence of noise sources. The comparison is illustrated by comparing the performance of the quantum Fourier transform and quantum phase estimation algorithms under a wide range of single- and twoqubit noise sources. Indeed, we obtain that when the different noise channels usually present in superconducting quantum processors are considered, the fidelity of these algorithms for the digital-analog paradigm outperforms the one obtained for the digital approach. Additionally, this difference grows when the size of the processor scales up, making DAQC a sensible alternative paradigm in the NISQ era. Finally, we show how to adapt the DAQC paradigm to quantum error mitigation techniques for canceling different noise sources, including the bang error.

I. INTRODUCTION

The origin of quantum computing dates back to 1980 when Benioff [1] suggested the use of quantum systems for traditional (reversible) computation, implementing a Turingmachine equivalence to unitary evolution. Simultaneously Manin [2], and a couple of years later Feynman [3], pointed out the convenience of quantum simulators to reproduce quantum problems. It was not until 1985 when Deutsch [4] proposed the idea of quantum gate, which led to the gate-based quantum computation model, known as the digital quantum computing (DQC) paradigm.

DQC is based on the use of digital pulses to perform quantum operations on the qubits, represented by means of singlequbit gates (SQG's), two-qubit gates (TQG's), and measurements. While DOC is the most outspread paradigm, there are other alternatives based on analog resources. One of the most promising ones is called adiabatic quantum computation or quantum annealing [5, 6]. Besides these paradigms, digitalanalog quantum computing (DAQC) is created from merging the digital and analog paradigms, combining the adaptability of DQC with the robustness of analog resources [7]. This universal paradigm is based on the application of digital and analog blocks to implement quantum circuits in a quantum computer. The digital steps consist of SQG's, while analog blocks are constructed via the time evolution of the natural interacting Hamiltonian provided by the quantum processor. There are several works that employ this paradigm either to simulate quantum many-body systems [8, 9] or to implement long depth quantum algorithms [10, 11].

Since the inception of quantum computing, a great deal of effort has been put into the development of the area. There is a great variety of hardware backends suitable for the performance of quantum computation, such as trapped ions [12] or superconducting circuits. The latest stands out as one of the most promising techniques to construct a quantum computer. They are solid-state electric circuits that use Josephson tunnel junctions, a highly non-linear and non-dissipative circuit element at low temperatures [13].

Noise is undoubtedly the main drawback in the scalability of quantum computing. Indeed, quantum computers cannot be completely isolated from the environment and the interactions performing quantum operations cannot be fully controlled, leading to decoherence, control errors, and crosstalk. Due to the limitations imposed by these error sources, a huge effort has been made to analyze them and propose quantum protocols more resistant to noise or capable of mitigating their effects [14, 15]. The most promising long-term solution for the scalability of quantum computers is the use of quantum error correction techniques [16, 17]. However, the current Noisy Intermediate-Scale Quantum (NISQ) [18, 19] era technology is not sufficient to implement quantum error correction to eliminate the undesired effect of noise sources in them.

A possibility to reduce the effect of noise sources in the era of NISQ devices is to adapt the quantum computing paradigm. Although the gate-based approach is the most extended paradigm, it is highly affected by noise. However, the effect is different depending on the type of gate. Indeed, it is almost negligible in SQG's, since they are fast and highly controllable. The length of TQG's makes them more exposed to decoherence, which together with the errors introduced by the indirect control and the crosstalk among qubits, turn these

^{*} Corresponding author: paula.garcia@iff.csic.es

[†] Corresponding author: mikel.sanz@ehu.es

gates very sensitive to noise. DAQC emerges as a sensible alternative quantum paradigm to overcome this problem within the NISO era limitations. This paradigm employs the natural interaction of the quantum processor to perform entangling operations and the running time of this Hamiltonian as an extra resource [20]. Consequently, the crosstalk among qubits and the control errors associated with switching on and off interactions are no longer a source of noise, but a resource, turning the problem of noise in TOG's into an advantage. Indeed, this approach has been numerically demonstrated to be more advantageous under the effect of certain experimental noise sources when compared to DOC [10]. However, to determine if DAQC is a suitable alternative to DQC in the NISQ era, a complete comparison of the performance of these paradigms comprising most of the noise sources present in superconducting quantum computers must be carried out.

In this Article, we perform a detailed comparison of the performance of DQC and DAQC paradigms under a wide range of noise sources, including thermal decoherence, bit-flip, measurement errors, and control errors. We first resort to the quantum Fourier transform (QFT), an important quantum subroutine with applications in multiple quantum algorithms [21–25]. The numerical study is performed for quantum processors of up to 6 qubits comparing the fidelity of the resulting state of the different paradigms to the exact solution. The results conclude that the banged DAQC paradigm shows a better tolerance to the most relevant noise sources present in superconducting quantum computers. This improvement becomes more relevant when the number of qubits scales up, allowing in principle for more accurate implementation of quantum algorithms in the NISQ era when compared to DQC.

To expand this analysis to more complex algorithms we choose the quantum phase estimation (QPE). Given a unitary operator U that has an eigenvector $|u\rangle$ with eigenvalue $e^{2\pi i \varphi}$, this algorithm estimates the unknown phase φ , and hence has multiple applications, such as in the Shor's [16] and Harrow-Hassidim-Lloyd algorithms [24]. This algorithm includes the inverse QFT besides some conditional rotations and SQG's, so we expect it to pose a greater challenge to the paradigms due to the greater effect of decoherence and other noise sources associated with the greater number of quantum gates. However, despite these larger noise sources, we show how using the DAQC paradigm we can approximate the exact solution with fidelities overcoming those of DQC.

We have organized the structure of the manuscript as follows. We start by explaining the fundamentals of DAQC in section II. In section III, we introduce the theoretical description of some of the most relevant noise sources present in current superconducting quantum computers. The comparison between the performance of DQC and DAQC is carried out in section IV using the QFT and QPE algorithms for the benchmark. In section V, we successfully apply error mitigation techniques to the DAQC paradigm, which allows us to cancel both decoherence and bang errors. Finally, in section VI, the conclusions and future perspectives of this work are discussed.

II. DIGITAL-ANALOG QUANTUM COMPUTING

In Ref. [7], Parra-Rodriguez *et al.* introduced a paradigm of quantum computation called DAQC. A DAQC algorithm combines elementary SQG's, performed with high accuracy with current technology, with entangling natural interactions among qubits in the processor. In addition to superconducting circuits [26], this paradigm of computation can be straightforwardly adapted to other quantum platforms such as trapped ions [27], Rydberg atoms [28], or nuclear magnetic resonance [29, 30].

In a superconducting quantum processor, digital blocks are implemented by short microwave pulses, while the analog blocks are derived from the qubit-to-qubit capacitive or inductive coupling. This interaction depends on the type of coupling, the topology of the architecture, or the nature of the qubit, among other aspects, but it can be generally expressed as a spin Hamiltonian. In our case, for the sake of simplicity, we have chosen a homogeneous all-to-all (ATA) Ising Hamiltonian. Although, in the case that qubits were coupled by an arbitrary inhomogeneous nearest-neighbor Ising Hamiltonian, it is possible to generate an arbitrary all-to-all Ising Hamiltonian only by employing single-qubit rotations [31]

$$H_0 = H_{\text{int}} = g \sum_{j < k}^{N} Z^{(j)} Z^{(k)} \rightarrow U_{\text{int}}(t) = e^{itH_{\text{int}}}, \quad (1)$$

where g is the coupling constant among qubits and $Z^{(i)}$ is the Pauli matrix $\sigma_z^{(i)}$ applied on the i-th qubit. However, the DAQC paradigm can be adapted to other emergent Hamiltonians, resulting in a universal paradigm for essentially all of them.

The homogeneous ATA two-body Ising Hamiltonian is a particular case of the inhomogeneous version,

$$H_{ZZ} = \sum_{j < k}^{N} g_{jk} Z^{(j)} Z^{(k)}, \text{ with } U_{ZZ} = e^{it_F H_{ZZ}},$$
 (2)

where now the coupling constant g_{jk} is different for each pair of qubits. For the sake of completeness, let us review the method introduced in Ref. [7]. Our first goal is to construct an arbitrary inhomogeneous Hamiltonian employing a combination of the aforementioned SQG's and analog blocks. Indeed, we can represent the evolution U_{ZZ} of an N-qubit inhomogeneous ATA two-body Ising Hamiltonian by N(N-1)/2 time slices $U_{\rm int}$ with times $\{t_{jk}\}_{j < k}^N$, where j,k are the indices of the application of the Z gates. More specifically, the analog block $U_{\rm int}(t_{nm})$ is sandwiched by $X^{(n)}X^{(m)}$ rotations. The map between both pictures is

$$H_{ZZ} = \sum_{j < k}^{N} g_{j,k} Z^{(j)} Z^{(k)}$$

$$= \frac{g}{t_F} \sum_{i < k}^{N} \sum_{n < m}^{N} t_{nm} X^{(n)} X^{(m)} Z^{(j)} Z^{(k)} X^{(n)} X^{(m)}.$$
(3)

Let us now see how the times t_{nm} must be chosen. Pauli matrices verify $\{\sigma_i,\sigma_j\}=2\delta_{ij}\mathbb{I}$ for i=x,y,z, so for

a term of the type $Z^{(k)}X^{(n)}$, it holds that $Z^{(k)}X^{(n)}=(-1)^{\delta_{kn}}X^{(n)}Z^{(k)}$, and analogously for the other terms. Using this we can write Eq. 3 as

$$H_{ZZ} = \frac{g}{t_F} \sum_{j < k}^{N} \sum_{n < m}^{N} t_{nm} (-1)^{\delta_{nj} + \delta_{nk} + \delta_{mj} + \delta_{mk}} Z^{(j)} Z^{(k)}.$$
(4)

This leads to a determined system of N(N-1)/2 linear equations, where the unknowns are the time steps of the analog blocks. The value of each time t_{nm} is given by the matrix inversion problem

$$g_{\beta} = t_{\alpha} M_{\alpha\beta} \frac{g}{t_F} \rightarrow t_{\alpha} = (M^{-1})_{\alpha\beta} g_{\beta} \frac{t_F}{q},$$
 (5)

where $M_{\alpha\beta}$ is a doubly stochastic matrix with elements ± 1 , $M_{\alpha\beta}=(-1)^{\delta_{nj}+\delta_{nk}+\delta_{mj}+\delta_{mk}}.$ The new indexes α and β are introduced to vectorize each pair of indexes (j,k) and (n,m) as

$$\alpha = N(n-1) - \frac{n(n+1)}{2} + m,$$
 (6)

$$\beta = N(j-1) - \frac{j(j+1)}{2} + k. \tag{7}$$

This matrix is invertible $\forall N \in \mathbb{Z} - \{4\}$ [8].

The method described is called stepwise DAQC (sDAQC) and it is universal and, therefore, equivalent to DQC. However, it shows the disadvantage that the analog blocks must be switched on and off, which induces important control errors. There is another paradigm called banged DAOC (bDAOC) in which the interaction Hamiltonian is never switched off and single-qubit rotations (SQR's) are applied on top of the analog dynamics. This introduces an inherent error, since it does not implement the exact algorithm, but when experimental errors are taken into account, it happens to scale up better than sDAQC and DQC [10, 11, 22]. This intuitively holds when the application time of SQRs, Δt , is much smaller than the time scale of the analog blocks, so the error introduced is smaller than the one coming from switching on and off the Hamiltonian in sDAQC. Indeed, experimentally, switching the interaction is not an exact step function and it takes some time to stabilize. A scheme of the implementation of both sDAQC and bDAQC is shown in Fig. 1.

III. THEORETICAL DESCRIPTION OF THE EFFECT OF NOISE SOURCES IN QUANTUM SYSTEMS

Quantum computers are open quantum systems, i.e., they cannot be completely isolated from the environment, and thus, they are susceptible to the noise caused by the control and the interaction with the environment. In general, the noise sources depend on the experimental setup used to run the quantum experiments. Our theoretical treatment of noise will employ the quantum channel formalism, in particular the operatorsum representation. In this formalism, the state of a quantum system is represented by a density matrix ρ . The general description of a quantum channel is a linear application, a

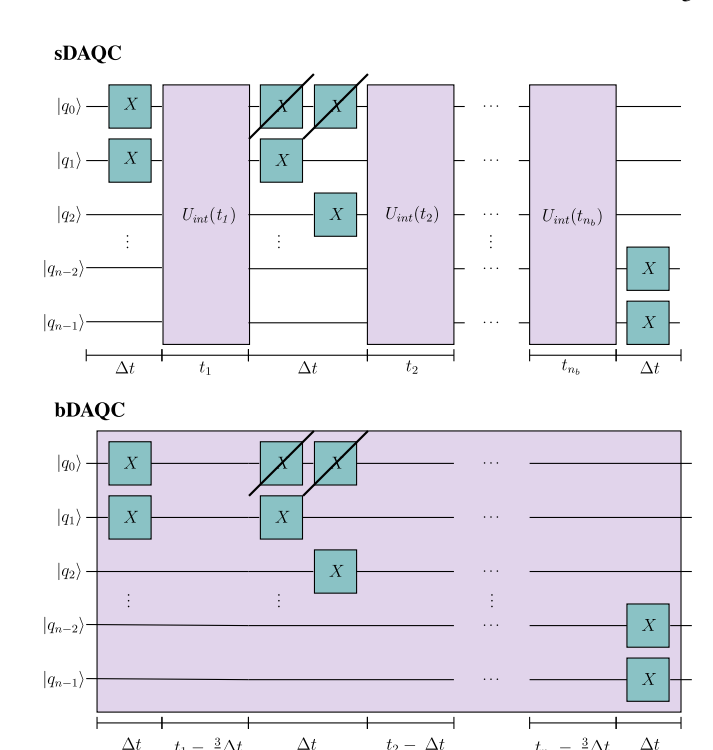


FIG. 1. Scheme of the implementation of the sDAQC and bDAQC paradigms. The analog blocks are depicted in purple and represent the interaction given by $U_{\rm int}$ in Eq. 1. The digital blocks are the blue ones, given by X gates. We can observe that in bDAQC, the digital blocks act on top of the analog interaction, while for sDAQC this interaction is turned on and off alternating with the digital blocks.

completely-positive-trace-preserving map \mathcal{E} , which maps the initial state ρ into the final one ρ' , i.e.,

$$\rho' = \mathcal{E}(\rho). \tag{8}$$

It encloses the change in the dynamics of the system by the application of an operator which describes a physical process [32]. These processes are, for example, the application of a quantum operation on a qubit or the de-excitation of a state due to the interaction with the environment.

The operator-sum representation is a rigorous mathematical formalism for quantum channels. Let us suppose that we have an open quantum system comprising our system of interest S and the environment E, with Hilbert spaces \mathcal{H}_S and \mathcal{H}_E , respectively, and $\{|e_k\rangle\}$ is an orthonormal basis for the finite-dimensional Hilbert space corresponding to the environment. Let us assume that the initial state of the environment is $\rho_{\text{env}} = |e_0\rangle\langle e_0|$. For the transformation U, the quantum operation can be written as [32]

$$\mathcal{E}(\rho) = \operatorname{tr}_{\text{env}} \left[U \left(\rho \otimes |e_0\rangle \langle e_0| \right) U^{\dagger} \right]$$

$$= \sum_{k} \langle e_k | U \left(\rho \otimes |e_0\rangle \langle e_0| \right) U^{\dagger} |e_k\rangle$$

$$= \sum_{k} E_k \rho E_k^{\dagger},$$
(9)

where $E_k \equiv \langle e_k | U | e_0 \rangle$ is an operator which acts on the subspace of the system. The operators E_k are called Kraus operators [33] and they play a key role in the description of the effect of noise sources in quantum systems.

Noise channels are non-unitary quantum channels that reproduce the effect of noise in the state of the system of interest, in our case the qubits comprising a quantum computer. Let us first focus on single-qubit quantum channels, which are those that only act on one qubit. More concretely, we study the noise channels that account for the three most common noise sources in superconducting quantum processors. These are bit-flip, decoherence, and measurement error.

The bit-flip channel is a model for errors in which the state of the qubit is randomly switched with a probability p and it is also present in classical computers. The energy to cause the flip of the qubit can be accidentally provided by pulses used to control the qubits or by thermal fluctuations. The Kraus operators of the bit-flip channel are

$$E_0 = \sqrt{1-p} \begin{pmatrix} 1 & 0 \\ 0 & 1 \end{pmatrix} = \sqrt{1-p} \mathbb{I}, \tag{10}$$

$$E_1 = \sqrt{p} \begin{pmatrix} 0 & 1 \\ 1 & 0 \end{pmatrix} = \sqrt{p}X, \tag{11}$$

where p is the bit-flip probability, \mathbb{I} is the 2×2 identity matrix and X is the σ_x Pauli matrix. When the measurement of the system is performed, the qubits might be affected by a bit-flip error. Based on this idea, we will introduce the measurement error as a bit-flip error preceding a perfect measurement operation.

Decoherence is represented through the generalized amplitude-damping channel. This quantum channel accounts for the de-excitation of a two-level system, i.e., the loss of amplitude of the excited state $|1\rangle$ that will decay into the ground state $|0\rangle$ with probability p. It can describe different physical phenomena related to energy dissipation such as the spontaneous emission of a photon and the scattering and attenuation of the state of a photon in a cavity, among others [32]. The Kraus operators of the generalized amplitude-damping channel are

$$E_0 = \sqrt{p} \begin{pmatrix} 1 & 0 \\ 0 & \sqrt{1 - \gamma} \end{pmatrix},\tag{12}$$

$$E_1 = \sqrt{p} \begin{pmatrix} 0 & \sqrt{\gamma} \\ 0 & 0 \end{pmatrix}, \tag{13}$$

$$E_2 = \sqrt{1-p} \begin{pmatrix} \sqrt{1-\gamma} & 0\\ 0 & 1 \end{pmatrix}, \tag{14}$$

$$E_3 = \sqrt{1 - p} \begin{pmatrix} 0 & 0 \\ \sqrt{\gamma} & 0 \end{pmatrix}, \tag{15}$$

where the stationary state of the environment is

$$\rho_{\text{env}} = \begin{pmatrix} p & 0\\ 0 & 1 - p \end{pmatrix},\tag{16}$$

with p the thermal population of the ground state.

The damping process can be understood as a time-accumulative problem, in which the probability grows with time [34]. It can be shown that γ can be written as $\gamma = 1 - e^{-t/T_1}$, where t is the time and T_1 is the thermal relaxation time and it describes processes due to the coupling of the qubit to its neighbors, which is a large system in thermal equilibrium at a temperature much higher than the one of the qubit [32].

Additionally, we also consider the control-related experimental errors described in Refs. [8, 10]. In this case, instead of a quantum-channel approach, we employ quantum trajectories [35]. The error due to SQG's is common to DQC and DAQC, as both use them as a resource to implement quantum algorithms. It simulates a uniform magnetic field noise affecting the qubits. It is given by the parameter ΔB , a random variable from a uniform probability distribution $\Delta B \in \mathcal{U}(1-r_D\Delta t/2,1+r_D\Delta t/2)$, where $\mathcal{U}(a,b)$ stands for a uniform noise distribution with range boundaries (a,b). The deviation ratio is given by r_D . This can be modeled as

$$e^{i\theta_k Z} \to e^{i\theta_k \Delta BZ},$$
 (17)

where Z stands for any SQG and θ_k is the rotation angle.

The noise due to the interaction among qubits is modeled in a different manner for DQC and DAQC. In DQC, any TQG can be decomposed in terms of CZ gates and SQG's. As the CZ gate can be written in terms of SQG's and ZZ interactions of the type described in Eq. 22, the effects of noise in any TQG can be modeled using the magnetic field noise for SQG's and a Gaussian phase noise for the two-qubit ZZ interaction. This Gaussian phase noise is represented by a random parameter $\varepsilon \in \mathcal{N}(0,\sigma_D)$ affecting the phase of the interaction, where $\mathcal{N}(\mu,\sigma)$ stands for a Gaussian distribution with mean μ and standard deviation σ . Its effect on a fixed $\pi/4$ phase interaction, which is usually the interaction of a digital quantum computer, is described by the change

$$e^{i\frac{\pi}{4}ZZ} \rightarrow e^{i\frac{\pi}{4}(1+\varepsilon)ZZ}$$
. (18)

For the DAQC paradigm, a Gaussian coherent noise affecting the time of the analog blocks is introduced to simulate the control error. It produces a switch in the time from $t_{\alpha} \rightarrow t_{\alpha} + \delta$, where $\delta \in \mathcal{N}(0, r_b \Delta t)$, with r_b the deviation ratio of the time Δt required for a single-qubit rotation. This can be implemented as

$$e^{it_{\alpha}H_{\text{int}}} \rightarrow e^{i(t_{\alpha}+\delta)H_{\text{int}}},$$
 (19)

where $H_{\rm int}$ is the natural interacting Hamiltonian of the quantum processor.

The parameters ε , ΔB , and δ must be chosen for each case and individually adapted to the different situations. The Gaussian coherent phase noise has a greater value for sDAQC than for bDAQC, as a result of the effect of switching on and off the interaction in sDAQC, as explained in section II. The value of these parameters changes each time a gate is applied to the circuit, as the effects of the noise described can vary in each application.

IV. IMPLEMENTATION OF A NOISE MODEL USING THE DQC AND DAQC PARADIGMS

In this section, we illustrate the noise model described in section III with the QFT and QPE algorithms.

A. Quantum Fourier transform

In Ref. [10] is shown that the N-qubit QFT can be written as a series of unitary gates of the form

$$U_{\text{QFT}} = \left[\prod_{m=1}^{N-1} U_{\text{SQG},m} U_{\text{TQG},m} \right] \cdot U_{H,N}, \tag{20}$$

where

$$U_{\text{SQG},m} = \exp\left[i\sum_{k=2}^{N-(m-1)} \theta_k \left(\mathbb{I} - Z^{(k+m-1)} - Z^{(m)}\right)\right] \times \left[i\pi\left(-Z^{(m)} + Y^{(m)}\right)\right]$$

$$\times \exp\left[\frac{i\pi}{2}\left(\mathbb{I} - \frac{Z^{(m)} + X^{(m)}}{\sqrt{2}}\right)\right],\tag{21}$$

$$U_{\text{TQG}} = \exp\left(i\sum_{c< k}^{N} \alpha_{c,k,m} Z^{(c)} \otimes Z^{(k)}\right), \tag{22}$$

$$U_{H,m} = \exp\left(\frac{i\pi}{2} \left[\mathbb{I} - \frac{(Z^{(m)} + X^{(m)})}{\sqrt{2}} \right] \right),$$
 (23)

$$\theta_k = \frac{\pi}{2^{k+1}}$$
 and $\alpha_{c,k,m} = \delta_{c,m} \frac{\pi}{2^{k-m+2}}$, (24)

where the superindices in brackets determine onto which qubit the gate acts. In order to obtain the total unitary, we compute the tensor product with the identity until dimension 2^N is reached.

The entangling gates of the algorithm are described by Eq. 22, which is the unitary representation of an inhomogeneous ATA two-body Ising Hamiltonian. The DQC paradigm decomposes the entangling gate into fixed $\pi/4$ phase inhomogeneous ATA two-body Ising Hamiltonians as

$$e^{i\alpha_{c,k,m}Z^{c}Z^{k}} = e^{i\frac{\pi}{4}Y^{c}} e^{i\frac{\pi}{4}Z^{c}Z^{k}} e^{i\alpha_{c,k,m}Y^{c}} X^{k}$$

$$\times e^{i\frac{\pi}{4}Z^{c}Z^{k}} X^{k} e^{-i\frac{\pi}{4}Y^{c}}.$$
(25)

where the phase $\alpha_{c,k,m}$ is the coefficient in Eq. 24.

To obtain a fair comparison of the performance of DQC, sDAQC, and bDAQC for the implementation of the QFT, we choose a series of initial states from the family of states $|\psi_0\rangle=\sin\beta\,|W_N\rangle+\cos\beta\,|GHZ_N\rangle$, where $\beta\in[0,\pi]$. The comparison is performed for the 3-, 5- and 6-qubit QFT so we can observe the effect of the noise sources as the number of qubits increases.

The noise model that we consider encloses the most relevant noise sources in superconducting quantum computers: bit-flip, decoherence, and measurement error, as well as control-related errors such as magnetic field fluctuations.

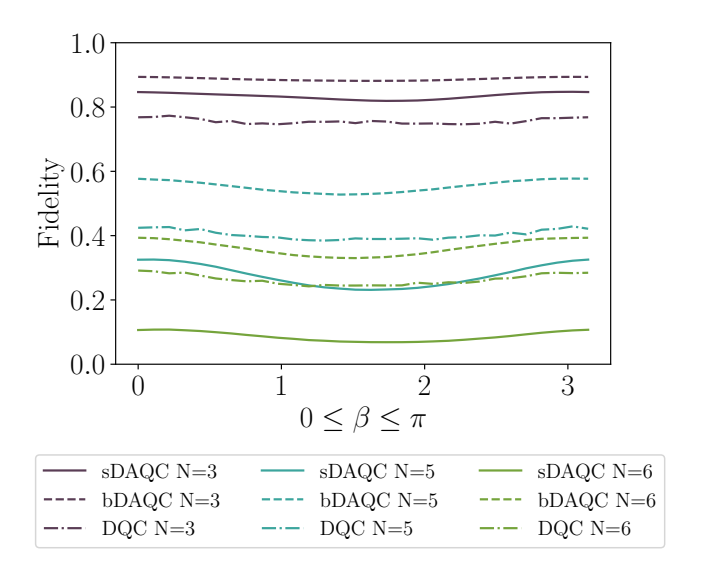


FIG. 2. Fidelity of the implementation of the 3-, 5- and 6-QFT algorithm to the family of states $|\psi_0\rangle=\sin\beta\,|W_N\rangle+\cos\beta\,|GHZ_N\rangle$ using the DQC, sDAQC and bDAQC paradigms. The highest fidelity is obtained for the bDAQC protocol. DAQC presents a better tolerance to decoherence than DQC due to the shorter time of application of the analog blocks with respect to TQG's. Moreover, the effect of bit-flip error in bDAQC is smaller than on sDAQC as the analog interaction is always on, so the bit-flip only affects SQRs in bDAQC, as opposed to sDAQC in which all the qubits of the system are subjected to it when an analog block is applied.

However, the difference in the implementation of the entangling blocks in DQC and DAQC leads to a different experimental error associated with them, which is modeled as a Gaussian phase noise on the application time of the TQG's in DQC and the analog blocks in DAQC.

The figure of merit used for the comparison is the fidelity

$$F(\rho_{\text{ideal}}, \rho_{\text{noisy}}) = \left[\text{tr} \left(\sqrt{\sqrt{\rho_{\text{ideal}}} \rho_{\text{noisy}} \sqrt{\rho_{\text{ideal}}}} \right) \right]^2, \quad (26)$$

where $ho_{\rm ideal}$ is the ideal state after the application of the QFT, while $ho_{\rm noisy}$ is the resulting state when the noise model is implemented. The fidelity verifies $0 \leq F(\rho_{\rm ideal}, \rho_{\rm noisy}) \leq 1$, and the larger the values the more similar are $ho_{\rm ideal}$ and $ho_{\rm noisy}$.

The values of the parameters used to simulate the different noise sources are chosen to model realistic NISQ superconducting devices. For the experimental errors described in Ref. [10], we select the values proposed by the authors. The magnetic field noise acting on single-qubit gates is given by a uniform probability distribution $\mathcal{U}(1-\text{SQGN},1+\text{SQGN})$, with SQGN = 0.0005. For the entangling blocks, for both DQC and DAQC, the noise is modeled by a random variable from a Gaussian distribution $\mathcal{N}(0,\sigma)$. The value of the standard deviation σ depends on the paradigm used. For DQC, the standard deviation is TQGN= 0.2000, while for DAQC we have sABN= $0.0200/g_0$ and bABN= $0.0100/g_0$, for sDAQC and bDAQC, respectively. The parameter g_0 is the coupling

constant of the homogeneous ATA two-body Ising Hamiltonian of the analog blocks and it is equal to 10 MHz. On the other hand, for the incoherent noise models introduced in Section III, we have a bit-flip error with probability $p_{\rm b-f}=0.005$ and a measurement error with probability $p_{\rm meas}=0.01.$ Notice that measurement error is currently a great technological limiting factor for quantum algorithms run in superconducting quantum processors. Finally, for the decoherence channel, the relaxation time T_1 is $50~\mu \rm s$, with thermal population of the ground state p=0.35. The length of the SQG's is $\Delta t_{\rm SQG}=1/(100g_0)$, while for the two-qubit interaction it is $\Delta t_{\rm TQG}=(1+\varepsilon)100\Delta t_{\rm SQG}\pi/4$ for TQG's, and for the analog blocks, it is the one obtained from the decomposition of the interaction.

The simulation using the previous values of the parameters is depicted in Fig. 2, averaged over 1000 repetitions to obtain a sufficiently good statistical sample. We can conclude that the bDAQC protocol shows better performance when the noise sources considered by our noise model are taken into account. Although for the ideal case the lowest fidelity results are obtained for bDAQC [10], in the noisy simulation, we observe that it shows the best tolerance to errors. The reason is that the error due to turning on and off the interaction overcomes the inherent error of the bDAQC introduced by having the interaction always on. Moreover, the fact that the interaction is never switched off also makes bDAOC only affected by the bit-flip error for the SQG's, so no bit-flip error is introduced due to the entangling blocks as it does in both DQC and sDAQC. For the chosen set of parameters, the total time of application of the QFT algorithm using the DAQC paradigm is shorter than the total time using DQC. Therefore, the DAOC paradigm is less affected by decoherence than the DOC paradigm. The measurement error is common for the three paradigms, so its effect in the fidelity is reflected as a shift in all the values. The performance of the QFT algorithm decreases fast with the number of qubits due to the increase in depth of the algorithm, as the number of gates is of order $\mathcal{O}(N^2)$, where N stands for the number of qubits. Thus, under a fair comparison considering the experimental values and the same noise sources, bDAQC obtains the highest value of fidelity.

Although we have chosen the QFT algorithm for our comparison, it allows us to extend the results to any general quantum algorithm, as the noise sources considered are independent of the algorithm implemented. In addition, if the scaling of the number of quantum gates with the number of qubits is slower than in the QFT, better fidelity results are expected.

B. Quantum phase estimation

To extend our study of the effect of noise sources in DQC and DAQC paradigms, we propose the QPE algorithm [32]. This algorithm estimates the phase φ that corresponds to the eigenvalue $e^{2\pi i \varphi}$ of the eigenvector $|u\rangle$ of a unitary operator U, where φ is unknown. In this algorithm, we use two quantum registers. In the first one, we use t qubits that determine the accuracy in the approximation of φ . The second register is

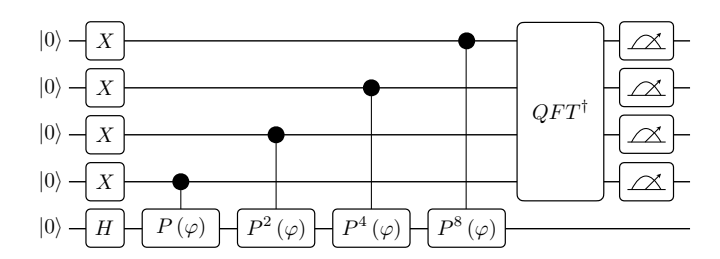


FIG. 3. QPE algorithm for $P\left(\varphi\right)$ (27), such that $P(\varphi)|u\rangle=e^{i2\pi\varphi}|u\rangle$. Hence, the final value of φ should be $\varphi=1/3$.

used to encode the eigenvector $|u\rangle$. Then, we initialize the first register by applying a Hadamard gate on each qubit, and then we apply a series of controlled rotations on the second register with U exponentiated to increasing powers of two. After that, we apply the inverse Fourier transform on the first register, which allows us to recover an approximation of φ , and hence the eigenvalue we were looking for.

In the previous section (Sec. IV A) we studied how the QFT's precision scales with the number of qubit using DQC, sDAQC and bDAQC under noisy circumstances. We observed that for a growing number of qubits, the DAQC paradigm outperforms DAQC. Therefore, as the inverse QFT is part of the QPE algorithm, we would expect it to have a similar performance. We propose to push the limits of these paradigms by obtaining a concrete eigenvalue via the QPE algorithm. This algorithm poses a greater challenge for the performance of DQC, as it includes a larger number of controlled two-qubit operations, which are the main noise source in current superconducting devices. Thus, we expect that the use of the analog evolution of DAQC allows us to obtain higher fidelities than in the digital approach.

Given the unitary operator $P(\varphi)$,

$$P\left(\varphi\right) = \begin{pmatrix} 1 & 0\\ 0 & e^{i2\pi\varphi} \end{pmatrix},\tag{27}$$

we aim at obtaining φ such that $P(\varphi)|u\rangle = e^{i2\pi\varphi}|u\rangle$. We choose a 4-qubit register to estimate the phase φ that corresponds to the eigenvector $|u\rangle = |1\rangle = (0 \quad 1)^T$. The complete QPE circuit is depicted in Fig. 3.

To implement this circuit we follow a different approach from the one for the QFT. In the previous algorithm, we tailored each quantum gate to obtain the best possible performance of the methods, for example, by combining and applying all quantum gates simultaneously on the same pulse, as described in Ref. [10]. However, in practical applications, quantum operations are reduced to a basis of quantum gates, each with a corresponding pulse, and all operations need to be rewritten in terms of them. Then, for the application of this algorithm, we propose to choose a concrete set of quantum gates based on the ones in a real superconducting quantum computer. We choose the universal set $\{R_x(\theta), R_z(\theta), \text{CNOT}\}$, and construct a tool to map the DQC circuit in the basis gates to the corresponding decomposition in the DAQC paradigm.

The developed tool simulates the noise sources in the quantum computer similar to the application to the QFT in Sec.

IV A, but uses a more general scheme capable of implementing a variety of algorithms. Moreover, it also considers the effect of residual signals in neighboring qubits when applying the pulses for a SQG (crosstalk), effectively applying the bit-flip error to all qubits after each digital block.

In our simulations, we have used noise parameters based on state-of-the-art quantum computers. In this case, we resort to approximated values of the execution times for the basis gates of IBM quantum computers, with $t_{R_r} = 10 \text{ns}$, $t_{R_z} = 1$ ns, and $t_{CNOT} = 300$ ns, which show that the execution time for TQGs is one or two orders of magnitude larger than the one of SQGs, which is consistent to each great effect to noise due to decoherence. The approximated error for these gates is of TQGN = 0.08, with CNOT = $e^{-isH_{\text{CNOT}}}$. where $s \in \mathcal{N}(\pi/2, TQGN)$. This error has been also estimated from real IBM devices. We choose a 0.0001 bit-flip probability for SQGs, and the same value as before for the error measurement, $p_{\text{meas}} = 0.01$. Regarding decoherence, we consider a T_1 time of 50μ s with thermal population of the ground state p = 0.35. Finally, for the experimental errors defined in Ref. [10] we use SQGN = 0.0005, sABN = 0.002, and bABN = 0.001. The coupling strength in these simulations has been chosen to be $g_0 = 1$ (units of g_0).

We use these parameters to estimate the phase φ such that $P(\varphi)|u\rangle=e^{i2\pi\varphi}|u\rangle$, choosing $|u\rangle$ to be equal to $|1\rangle=$ $(0 1)^T$. In Fig. 4 we observe that under ideal circumstances, the higher probabilities are those of the 0101 and 0110 states, which lead to the approximations of φ , $\varphi_{0101} = 5/16 =$ 0.3125, $\varphi_{0110} = 6/16 = 0.375$, with a relative error of 6.25% and 12.5% respectively, with respect to the exact result $\varphi = 1/3$. We observe that even under noisy circumstances, we are capable of recovering the maximum probability states with both DQC and DAQC. Regarding the fidelity, we obtain $F(\rho_{\text{ideal}}, \rho_{\text{DQC}}) = 0.88$, $F(\rho_{\text{ideal}}, \rho_{\text{bDAQC}}) = 0.87$, and $F(\rho_{\text{ideal}}, \rho_{\text{sDAOC}}) = 0.79$. We observe that in this case DQC and bDAQC lead to similar values of fidelity. However, the bDAQC paradigm shows a better approximation of the solution, as the maximum probability peaks are closer to the ideal ones, which is consistent with the conclusions obtained from Sec. IV A.

V. ERROR MITIGATION IN DAQC

The effect of noise sources limits the performance of current NISQ processors [18]. Quantum error mitigation techniques emerge to successfully deal with these effects within the NISQ era [36–38]. Some of the latest proposals of error mitigation techniques apply the quasi-probability method stochastically to analog, DAQC, or DQC platforms and efficiently can eliminate errors [39, 40], or suppress algorithmic errors such as Trotter error [41]. Therefore, to show the actual performance of DAQC, it is necessary to show how to adapt quantum error mitigation techniques to this paradigm. In fact, we will demonstrate that these techniques can be successfully modified to cancel the intrinsic error associated with bDAQC.

We apply the zero noise extrapolation technique [42, 43], based on the extrapolation of the noisy results to the zero

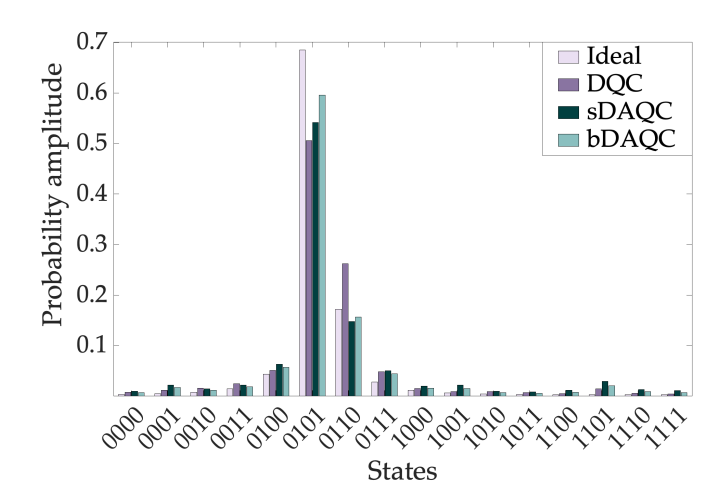
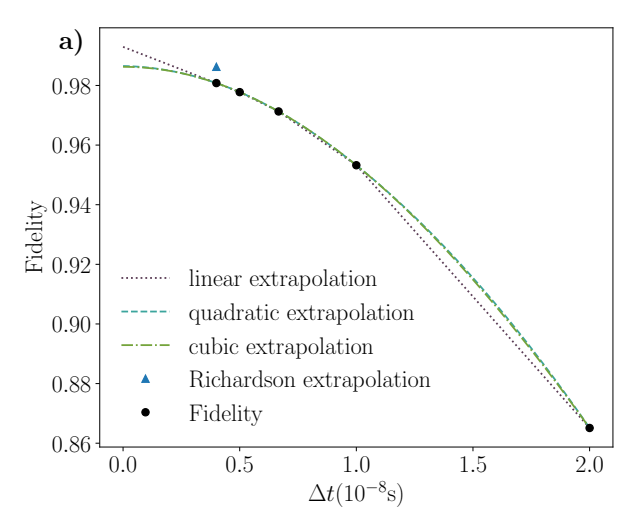


FIG. 4. **QPE results for DQC, sDAQC and bDAQC.** Probability amplitudes of the resulting states of the QPE algorithm for the considered paradigms and noise sources for $\varphi = 1/3$ and the unitary operator in Eq. (27).

noise limit. We consider only the effect of decoherence in the system and run the bDAQC QFT circuit for the initial state $|\psi_0\rangle=\sin\pi/4\,|\mathrm{W}_6\rangle+\cos\pi/4\,|\mathrm{GHZ}_6\rangle$, for different values of the coupling constant $g_j,\ j=0,\ldots,n_g$. This way, we modify the total time of the application of the circuit as $t_{j_\alpha}\propto g_j^{-1}$ and hence, the effect of decoherence. However, the variation of g_j also affects the intrinsic error of the bDAQC paradigm. In order to avoid this effect, we choose $\Delta t_{\mathrm{SQG}_{i,j}}=b_i/g_j$, as for a given g_j the time of the digital block is defined to be inversely proportional to the coupling constant. Then, for a certain number of values of g_j , it is possible to extrapolate the fidelity results to the zero decoherence limit-zero total time, removing the error due to decoherence.

Moreover, it is also possible to extend this technique to eliminate the intrinsic error introduced by bDAQC. In order to do that, we repeat the previous procedure for $i=0,...,n_t$ values of $\Delta t_{\mathrm{SQG}_{i,j}}=b_i/g_j$, employing the zero decoherence values to perform the extrapolation to the zero Δt_{SQG} limit. The result is the fidelity of the ideal circuit, both without the error due to decoherence and bDAQC (Fig. 5a). The best fidelity is obtained for the linear extrapolation and it is approximately 0.9929, which means that the error mitigated state is a great approximation of the ideal one.

However, it is not always possible to obtain the quantum state after the application of a quantum circuit, as it is a costly operation due to the use of tomography. Thus, in order to verify the performance of error mitigation for bDAQC, it is necessary to choose a second figure of merit that can easily be computed from the measurements of a quantum circuit. We choose the expectation value of the observable $Z_0 = Z \otimes \mathbb{I} \otimes \cdots \otimes \mathbb{I}$. The results are shown in Fig. 5b. We observe that the best approximation of $\langle Z_0 \rangle$ is approximately 0.2883, computed using Richardson extrapolation. The error $\varepsilon = |\langle Z_0 \rangle_{\text{ideal}} - \langle Z_0 \rangle_{\text{noisy}}| = 0.0003$ shows that we can obtain an extremely accurate approximation of the ideal expectation value from the noisy one.



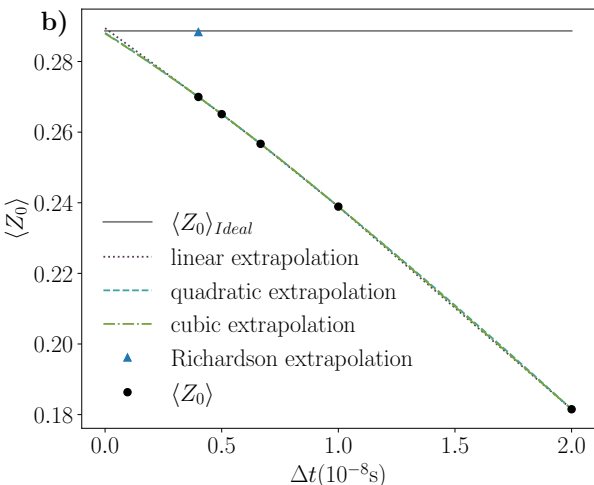


FIG. 5. Results of the error mitigation. (a) Fidelity, and (b) $\langle Z_0 \rangle$. Both fidelity and $\langle Z_0 \rangle$ attain extremely accurate approximations of the ideal values, especially for linear and Richardson extrapolation, respectively. The simulations where made for the 6-qubit QFT circuit with $T_1=50~\mu s$, p=0.35 and $g_0=1~\text{MHz}$.

The results obtained in Fig. 5 show that it is possible to recover the ideal results from the application of the bDAQC paradigm by resorting to zero noise extrapolation. Although we have focused on bDAQC, these results can be extended to sDAQC, as in this case only the zero decoherence limit would be studied. For a more detailed discussion of the error mitigation for bDAQC and concrete results see the Appendix.

VI. CONCLUSIONS AND PERSPECTIVES

The aim of this manuscript was to perform an exhaustive platform-based comparison between the DAQC and DQC paradigms in order to determine if DAQC is actually a sensi-

ble alternative paradigm in the NISQ era. With this in mind, we have illustrated the experiment by implementing the QFT algorithm, considering a noise model that comprises the most relevant noise sources in current superconducting quantum processors. From our simulations, we conclude that bDAQC is a suitable alternative for NISQ processors. For 3 qubits the fidelity is about 90% for bDAQC and 85% for sDAQC, while for DQC it is about 80%. As the number of qubits increases, we have observed that the fidelity values obtained for bDAQC still overcome considerably the ones of DQC, although sDAQC presents a worse performance, due to the increasing number of analog blocks affected by the bit-flip. For a higher number of qubits, the effect of the noise sources leads to fidelity values too low to obtain conclusive results from the output of the experiments.

We have also extended the application of the DAQC paradigm to a new algorithm never used in the DAQC literature, the QPE algorithm. This algorithm is a subroutine in important applications of quantum computing, and hence it is key to finding the optimum paradigm to minimize the errors. We have tested the performance of this algorithm under noise sources and we conclude that again, the bDAQC paradigm offers the better approximation to the ideal result.

Moreover, we have also proven that quantum error mitigation techniques can be adapted to the DAQC paradigm, reinforcing the proposal of this paradigm as an appropriate alternative to DQC in the NISQ era.

The results are highly encouraging for the development of NISQ computation architectures. As an outlook, this study can be extended to consider other noise channels, such as correlated noises, in order to match the performance of other architectures [44, 45], as well as the comparison of our predictions with actual implementations based on transmon or flux qubits.

ACKNOWLEDGEMENTS

The authors thank Juan José García-Ripoll for the useful discussions. The authors acknowledge support from Spanish MCIU/AEI/FEDER (PGC2018-095113-B-I00), Basque Government IT986-16, project grant PID2021-125823NA-I00 funded by MCIN/AEI/10.13039/501100011033, the projects QMiCS (820505) and OpenSuperQ (820363) of the EU Flagship on Quantum Technologies, the QUANTEK project (ELKARTEK program from the Basque Government, expedient no. KK-2021/00070), as well as "ERDF A way of making Europe" and "ERDF Invest in your Future". P.G.M. acknowledges support from MCIU/AEI/FEDER PGC2018-094792-B-I00, CSIC Research Platform PTI-001, the Proyecto Sinérgico CAM 2020 Y2020/TCS-6545 (NanoQuCoCM), and MCIN/AEI/10.13039/501100011033 and "FSE invierte en tu futuro" through an FPU Grant. FPU19/03590. M.G.d.A. acknowledges support from the UPV/EHU and TECNALIA 2021 PIF contract call. M.S. acknowledges support from Spanish Ramón y Cajal Grant RYC-2020-030503-I.

- [1] P. Benioff, The computer as a physical system: A microscopic quantum mechanical Hamiltonian model of computers as represented by Turing machines. Journal of Statistical Physics 22, 563 (1980).
- [2] Y. I. Manin, *Vychislimoe i nevychislimoe*. Sov. Radio, 13 (1980).
- [3] R. P. Feynman, *Simulating physics with computers*. International Journal of Theoretical Physics **21**, 467 (1982).
- [4] D. Deutsch, Quantum theory, the Church–Turing principle and the universal quantum computer. Proceedings of the Royal Society A 400, 97 (1985).
- [5] E. Farhi, J. Goldstone, S. Gutmann, and M. Sipser, *Quantum Computation by Adiabatic Evolution*. ArXiv: quant-ph/0001106 (2000).
- [6] T. Albash and D. A. Lidar, Adiabatic quantum computation. Rev. Mod. Phys. 90, 015002 (2018).
- [7] A. Parra-Rodriguez, P. Lougovski, L. Lamata, E. Solano, and M. Sanz, *Digital-Analog Quantum Computation*. Physical Review A 101, 022305 (2020).
- [8] L. Lamata, A. Parra-Rodriguez, M. Sanz, and E. Solano, Digital-analog quantum simulations with superconducting circuits. Advances in Physics: X 3 1457981 (2018).
- [9] L. C. Céleri, D. Huerga, F. Albarrán-Arriagada, E. Solano, and M. Sanz, *Digital-analog quantum simulation of fermionic mod*els. ArXiv: 2103.15689 (2021).
- [10] A. Martin, L. Lamata, E. Solano, and M. Sanz, *Digital-analog quantum algorithm for the quantum Fourier transform*. Physical Review Research 2, 013012 (2020).
- [11] D. Headley, T. Müller, A. Martin, E. Solano, M. Sanz, and F. K. Wilhelm, Approximating the Quantum Approximate Optimisation Algorithm. ArXiv:2002.12215 (2021).
- [12] J. I. Cirac and P. Zoller, Quantum Computations with Cold Trapped Ions. Physical Review Letters 74, 4091 (1995).
- [13] M. H. Devoret, A. Wallraff, and J. M. Martinis, Superconducting Qubits: A Short Review. ArXiv:cond-mat/0411174 (2004).
- [14] Y. Zhang, H. Deng, Q. Li, H. Song, and L. Nie, Optimizing Quantum Programs Against Decoherence: Delaying Qubits into Quantum Superposition. 13th International Symposium on Theoretical Aspects of Software Engineering (TASE), July 29 -August 1, (2019).
- [15] M. Sarovar, T. Proctor, K. Rudinger, K. Young, E. Nielsen, and R. Blume-Kohout, *Detecting crosstalk errors in quantum infor*mation processors. Quantum 4, 321 (2020).
- [16] P. W. Shor, Scheme for reducing decoherence in quantum computer memory. Physical Review A 52, 2493 (1995).
- [17] C. H. Bennett, D. P. DiVincenzo, J. A. Smolin, and W. K. Wootters, *Mixed-state entanglement and quantum error correction*. Physical Review A 54, 3824 (1996).
- [18] J. Preskill, *Quantum Computing in the NISQ era and beyond*. Quantum **2**, 79 (2018).
- [19] K. Barthi, et al, Noisy intermediate-scale quantum algorithms. Reviews of Modern Physics 94, 015004 – Published 15 February 2022 (2022).
- [20] T. Gonzalez-Raya, R. Asensio-Perea, A. Martin, L. C. Céleri, M. Sanz, P. Lougovski, and E. F. Dumitrescu, *Digital-Analog Quantum Simulations Using The Cross-Resonance Effect*. PRX Quantum 2, 020328 (2021).
- [21] P. W. Shor, Polynomial-Time Algorithms for Prime Factorization and Discrete Logarithms on a Quantum Computer. SIAM Journal on Computing 26, 1484 (1996).

- [22] A. Martin, B. Candelas, Á. Rodríguez-Rozas, J. D. Martín-Guerrero, X. Chen, L. Lamata, R. Orús, E. Solano, and M. Sanz, *Toward Pricing Financial Derivatives with an IBM Quantum Computer*. Physical Review Research 3, 013167 (2021).
- [23] J Gonzalez-Conde, Á. Rodríguez-Rozas, E. Solano, and M. Sanz, Pricing Financial Derivatives with Exponential Quantum Speedup. ArXiv:2101.04023 (2021).
- [24] A. W. Harrow, A. Hassidim, and S. Lloyd, Quantum Algorithm for Linear Systems of Equations. Physical Review Letters 103, 150502 (2009).
- [25] S. Lloyd, M. Mohseni, and P. Rebentrost, Quantum principal component analysis. Nature Physics 10, 631 (2014).
- [26] J. Yu, J. C. Retamal, M. Sanz, E. Solano, and F. Albarrán-Arriagada, Superconducting Circuit Architecture for Digital-Analog Quantum Computing. ArXiv: 2103.15696 (2021).
- [27] D. Porras, and J. I. Cirac, Effective Quantum Spin Systems with Trapped Ions. Physical Review Letters 92, 207901 (2004).
- [28] A. W. Glaetzle, R. M. W. van Bijnen, P. Zoller, and W. Lechner, A coherent quantum annealer with Rydberg atoms. Nature Communications 8, 15813 (2017).
- [29] S. Lloyd, A Potentially Realizable Quantum Computer. Science **261**, 1569 (1993).
- [30] D. G. Cory, M. D. Price, and T. F. Havel, Nuclear magnetic resonance spectroscopy: An experimentally accessible paradigm for quantum computing. Physica D: Nonlinear Phenomena 120, 82 (1998).
- [31] A. Galicia, B. Ramon, E. Solano, and M. Sanz, Enhanced connectivity of quantum hardware with digital-analog control. Physical Review Research 2, 033103 (2020).
- [32] M. A. Nielsen and I. L. Chuang, *Quantum Computation and Quantum Information* (Cambridge University Press, Cambridge, 2010).
- [33] K. Kraus, States, Effects and Operations: Fundamental Notions of Quantum Theory (Springer Verlag, 1983).
- [34] J. Preskill, Lecture Notes for Ph219/CS219: Quantum Computation Chapter 3 (California Institute of Technology, 2018).
- [35] H. J. Carmichael, Quantum jumps revisited: An overview of quantum trajectory theory (Quantum Future From Volta and Como to the Present and Beyond. Lecture Notes in Physics, vol 517. Springer, Berlin, Heidelberg, 1999).
- [36] S. Endo, S. C. Benjamin, and Y. Li, Practical Quantum Error Mitigation for Near-Future Applications. Physical Review X 8, 031027 (2018).
- [37] A. Kandala, K. Temme, A. D. Córcoles, A. Mezzacapo, J. M. Chow, and J. M. Gambetta, *Error mitigation extends the com*putational reach of noisy quantum processor. Nature **567**, 491 (2019).
- [38] S. Endo, Z. Cai, S. C. Benjamin, and X. Yuan, Hybrid Quantum-Classical Algorithms and Quantum Error Mitigation . Journal of the Physical Society of Japan 90, 032001 (2021).
- [39] J. Sun, X. Yuan, T. Tsunoda, V. Vedral, S. C. Benjamin, and S. Endo, *Mitigating Realistic Noise in Practical Noisy Intermediate-Scale Quantum Devices*. Physical Review Applied 15, 034026 (2021).
- [40] S. Endo, Q. Zhao, Y. Li, S. Benjamin, and X. Yuan, *Mitigating algorithmic errors in a Hamiltonian simulation*. Physical Review X 99, 012334 Physical Review A (2019).
- [41] H. Hakoshima, Y. Matsuzaki, and S. Endo, *Relationship between costs for quantum error mitigation and non-Markovian measures*. Physical Review A **103**, 012611 (2021).

- [42] Y. Li and S. C. Benjamin, Efficient Variational Quantum Simulator Incorporating Active Error Minimization. Physical Review X 7, 021050 (2017).
- [43] K. Temme, S. Bravyi, and J. M. Gambetta, Error Mitigation for Short-Depth Quantum Circuits. Physical Review Letters 119, 180509 (2017).
- [44] L. Postler, Á. Rivas, P. Schindler, A. Erhard, R. Stricker, D. Nigg, T. Monz, R. Blatt, and M. Müller, Experimental quantification of spatial correlations in quantum dynamics. Quantum 2, 90 (2018).
- [45] A. Bermudez, X. Xu, M. Gutiérrez, S. C. Benjamin, and M. Müller, Fault-tolerant protection of near-term trapped-ion topological qubits under realistic noise sources. Physical Review A 100, 062307 (2019).

Appendix: ERROR MITIGATION

In section V we demonstrated how to apply error mitigation to the DAQC paradigm. In this appendix, we include a more detailed explanation of the procedure, as well as the values chosen for these simulations and the numerical results obtained.

First, in order to have a greater effect of the noise sources in our system, we choose $g_0=1$ MHz and only consider the effect of decoherence by means of the thermal relaxation channel with $T_1=50~\mu {\rm s}$ and p=0.35. We opt for a 6-qubit initial state $|\psi_0\rangle=\sin\pi/4~|{\rm W}_6\rangle+\cos\pi/4~|{\rm GHZ}_6\rangle$ and apply the bDAQC QFT circuit on it to study its delity and expectation value $\langle Z_0\rangle$ for different values of $\Delta t_{{\rm SQG}_{i,j}}=b_i/g_j$, with $b_i=[1/50,1/100,1/150,1/200,1/250]$ and $g_j=a_jg_0$, $a_j=[0.94,0.97,1.00,1.03,1.07]$.

The procedure is as follows. For each value of b_i , we perform a zero noise linear extrapolation with the time associated to each g_j as the noise parameter, leading to the zero decoherence limit for each b_i , i.e., $\Delta t_{\mathrm{SQG}_i} = b_i/g_0$, for the fidelity and the expectation value $\langle Z_0 \rangle$ (see Tables I-II). Using the zero decoherence limit values of these figures of merit we can move on to step two of the error mitigation for bDAQC, which is used to remove the intrinsic error associated with this paradigm. We use different extrapolation techniques and ob-

tain the results in Tables III-IV.

	b_0	b_1	b_2	b_3	b_4
g_0	0.7270	0.8006	0.8156	0.8211	0.8236
g_1	0.7312	0.8052	0.8204	0.8258	0.8284
g_2	0.7352	0.8096	0.8249	0.8303	0.8329
g_3	0.7390	0.8138	0.8291	0.8346	0.8372
g_4	0.7437	0.8190	0.8344	0.8400	0.8426
Zero decoherence limit	0.8651	0.9532	0.9713	0.9778	0.9808
Ideal	0.8771	0.9665	0.9848	0.9914	0.9945

TABLE I. Fidelity results for the first step of the zero noise extrapolation for bDAQC (zero decoherence).

	b_0	b_1	b_2	b_3	b_4
g_0	0.1692	0.2185	0.2337	0.2409	0.2451
g_1				0.2417	
g_2	0.1699	0.2197	0.2351	0.2424	0.2466
g_3	0.1703	0.2203	0.2357	0.2430	0.2473
g_4	0.1707	0.2210	0.2365	0.2439	0.2481
Zero decoherence limit	0.1815	0.2389	0.2567	0.2651	0.2700
Ideal	0.1813	0.2392	0.2571	0.2656	0.2705

TABLE II. $\langle Z_0 \rangle$ results for the first step of the zero noise extrapolation for bDAQC (zero decoherence).

Ideal	Linear	Cuadratic	Cubic	Richardson
1	0.9929	0.9865	0.9862	0.9863

TABLE III. Fidelity results for the second step of the zero noise extrapolation for bDAQC (zero Δt_{SOG}).

				Richardson
0.2887	0.2895	0.2881	0.2879	0.2883

TABLE IV. $\langle Z_0 \rangle$ results for the second step of the zero noise extrapolation for bDAQC (zero $\Delta t_{\rm SQG}$).